Evidence That Both Kinetic and Thermodynamic Factors Govern DNA Toroid Dimensions: Effects of Magnesium(II) on DNA Condensation by Hexammine Cobalt(III)†

Christine C. Conwell and Nicholas V. Hud*

School of Chemistry and Biochemistry, Parker H. Petit Institute of Bioengineering and Biosciences, Georgia Institute of Technology, Atlanta, Georgia 30332-0400

Received January 15, 2004; Revised Manuscript Received February 27, 2004

ABSTRACT: Millimolar concentrations of divalent cations are shown to affect the size of toroids formed when DNA is condensed by multivalent cations. The origins of this effect were explored by varying the order in which $MgCl_2$ was added to a series of DNA condensation reactions with hexammine cobalt chloride. The interplay between Mg(II), temperature, and absolute cation concentration on DNA condensation was also investigated. These studies reveal that DNA condensation is extremely sensitive to whether Mg(II) is associated with DNA prior to condensation or Mg(II) is added concurrently with hexammine cobalt(III) at the time of condensation. It was also found that, in the presence of Mg(II), temperature and dilution can have opposite effects on the degree of DNA condensation. A systematic comparison of DNA condensates observed in this study clearly illustrates that, under our low-salt conditions, toroid size is determined by the kinetics of toroid nucleation and growth. However, when Mg(II) is present during condensation, toroid size can also be limited by a thermodynamic parameter (e.g., undercharging). The path dependence of DNA condensation presented here illustrates that regardless of which particular factors limit toroid growth, toroids formed under the various conditions of this study are largely nonequilibrium structures.

In vitro condensation of DNA into toroidal structures by multivalent cations has been studied for over 25 years as a model of DNA condensation in living cells and viruses (*1*−*7*). Within the past decade, interest in understanding and controlling DNA condensation intensified with the pursuit of more efficient methods for artificial gene delivery (*8*−*11*). Many laboratories focused on the design and synthesis of new cationic molecules for the purpose of controlling condensate size and morphology (*12*). In contrast, relatively few experimental studies have addressed how DNA structure and solution conditions at the onset of condensation contribute to the size of the condensate particle (*13*−*19*).

Over the past several years, theoreticians have provided an in depth view of the attractive potential that causes DNA to condense in the presence of multivalent cations (*5*, *20*, *21*). However, uncovering the factors that govern DNA toroid size (i.e., thickness and diameter) has proven to be particularly challenging, especially because both thermodynamic and kinetic factors can contribute to limits on toroid growth. Under conditions of DNA condensation where there remains a free exchange of DNA strands between individual particles, the condensed DNA will eventually reach a thermodynamic equilibrium. In this situation, the size of DNA condensates should ultimately be determined by the buildup of a net electrostatic charge on each particle that is due to imperfect charge compensation between DNA and bound multivalent cations (*22*−*30*). However, under conditions where condensed DNA strands are not free to exchange between particles once condensation has initiated, particle size can be governed by the kinetics of condensation, which can in turn depend on salt conditions and DNA concentration (*19*, *31*, *32*).

We recently demonstrated that DNA toroid size increases substantially if the NaCl concentration in a DNA solution is increased from 1 to 10 mM prior to condensation with hexammine cobalt(III) (*19*). At low ionic strengths, condensates produced in the presence of $MgCl_2$ showed an increase in toroid size similar to the increase observed in samples containing NaCl at approximately the same ionic strength. We observed a further increase in mean toroid diameter for samples containing higher concentrations of $MgCl_2$ that could not be attributed solely to ionic strength, because a solution containing NaCl at the same ionic strength did not exhibit the same increase (*19*). Thus, at very low ionic strength, monovalent and divalent cations can have a similar influence on the formation of toroidal condensates. However, as ionic strength increases, cation valency also becomes an important parameter in determining condensate size. To the best of our knowledge, no other studies have systematically investigated the effects of salt concentrations below 10 mM on the formation of DNA toroids. It is somewhat surprising that such a fundamental parameter of DNA condensation was not previously investigated in detail, particularly since we have found millimolar changes in ionic strength to have a profound effect on the size of DNA condensates. Understanding the effects of ionic strength and cation valency on

† This work was supported by Research Grant GM62873 from the National Institutes of Health.

* To whom correspondence should be addressed. E-mail: hud@chemistry.gatech.edu.

10.1021/bi049872u CCC: $27.50
Published on Web 04/10/2004

DNA condensation is important for the preparation of DNA for gene delivery, because DNA particles are typically exposed to various salt conditions as they are condensed, encapsulated, and incorporated into cells. Additionally, such studies are valuable for elucidating the factors that govern toroid size under commonly used laboratory protocols for DNA condensation.

To further investigate the effects of Mg(II) on DNA condensation, we prepared a series of DNA condensation reactions in which the order of $MgCl_2$ addition was varied. These condensation reactions were carried out at both 22 and 37 °C. The effects of sample dilution after condensation were also explored to determine how varying the absolute, but not relative, concentration of different cations in the solution affects the integrity of DNA condensates. Transmission electron microscopy studies reveal the extent to which variations in the condensate structures are affected by the presence of Mg(II), particularly whether Mg(II) is associated with the DNA prior to condensation or it is added to the DNA concurrently with hexammine cobalt(III). Analyses of the observed effects of Mg(II) on particle size and morphology have allowed the development of models for the process of DNA toroid formation that illustrate how both kinetic and thermodynamic factors can determine toroid size.

EXPERIMENTAL PROCEDURES

DNA Preparation. Bluescript II SK− plasmid DNA (Stratagene, La Jolla, CA) was isolated from the *Escherichia coli* cell line DH5α (Life Technologies, Carlsbad, CA) using the Qiagen Maxi Prep kit (Valencia, CA). The DNA was eluted in 1× TE (10 mM Trizma base, pH 7.8, 1 mM EDTA). All DNA used was linearized by the restriction endonuclease *Hin*dIII (New England Biolabs, Beverly, MA), which singly cuts Bluescript II SK−. The DNA was rinsed using Microcon YM-30 spin columns (Millipore, Bedford, MA) at least five times with 0.25× TE to remove the buffer and salt from the restriction digest. The DNA was eluted from the spin column membrane to a final concentration of 20 μg/mL in 0.25× TE. Concentrations of DNA were verified spectrophotometrically. The DNA was prepared as two stock solutions: a low-salt solution in 1× TE and a solution containing 7.5 mM $MgCl_2$ in 1× TE.

Preparation of Condensation Solutions. DNA in solution was condensed by mixing with an equal volume of 200 μM hexammine cobalt chloride (Sigma, St. Louis, MO). Condensates were prepared such that $MgCl_2$ was introduced at three different stages of the condensation process: (1) DNA in solution with 3.5 mM $MgCl_2$ was condensed with hexammine cobalt chloride (preassociation of Mg(II)); (2) DNA was condensed with a hexammine cobalt chloride solution that contained 3.5 mM $MgCl_2$ (concurrent addition of $MgCl_2$); (3) $MgCl_2$ was added after the DNA was condensed with hexammine cobalt chloride in the absence of $MgCl_2$ (low-salt conditions). In all cases, DNA was allowed to condense for 5 min after mixing with the hexammine cobalt chloride solution. An aliquot was removed from the condensation reaction for examination by transmission electron microscopy (TEM). The remaining solution was diluted 2-fold with dH_2O, for samples in which $MgCl_2$ was already present, or with 1.75 mM $MgCl_2$ for the DNA condensates prepared in the absence of $MgCl_2$. These samples were allowed to equilibrate for an additional 10 min after dilution. The three diluted condensate solutions were identical in composition at 5 μg/mL DNA, 50 μM hexammine cobalt chloride, and 0.87 mM $MgCl_2$.

Transmission Electron Microscopy (TEM). Condensation mixtures were deposited on carbon-coated EM grids (Ted Pella, Redding, CA) and allowed to settle for 10 min. EM grids were stained by the addition of 2% uranyl acetate (Ted Pella) directly to the grid, then rinsed in 95% ethanol and air-dried. Condensation reactions and grid preparations were performed at 22 and 37 °C. Images of the condensates were collected on film using a JEOL-100C transmission electron microscope. All images were collected at 100 000× magnification.

RESULTS

Condensation Is Directly Affected by the Presence of $MgCl_2$. The morphology, size, and degree of aggregation of DNA condensates were examined as a function of $MgCl_2$ being added at different points during the condensation process. Under the first experimental conditions, a linear 3 kb DNA was condensed by hexammine cobalt chloride in the absence of $MgCl_2$. Condensates were produced by mixing a 20 μg/mL DNA solution in a low-salt buffer (1× TE, pH 7.8) with an equal volume of 200 μM hexammine cobalt chloride. These conditions will be referred to as "low-salt" condensation. The majority of the particles observed by TEM were well-defined toroids, although rods were occasionally observed (Figure 1A). The toroids in these preparations have a mean outside diameter of 77 nm and a mean hole diameter of 21 nm. These measurements are typical of toroids produced by the condensation of DNA from a low-salt solution (*19*, *33*).

In the second protocol, a 20 μg/mL DNA solution containing $MgCl_2$ (3.5 mM $MgCl_2$, 1× TE, pH 7.8) was mixed with an equal volume of 200 μM hexammine cobalt chloride. This condensation reaction produced toroidal structures that were predominately associated within small aggregates, typically containing three to ten toroids (Figure 1B). Additionally, toroids within these aggregates appear larger than those observed in the low-salt preparation that contained no divalent cations.

In the third condensation protocol, low-salt DNA was condensed by mixing with an equal volume of a solution containing both 200 μM hexammine cobalt chloride and 3.5 mM $MgCl_2$. The resulting condensates were toroid-like structures, but were dissimilar from any DNA toroids we had previously observed. These "super toroids", as we will refer to these particular condensates, were approximately three times larger than toroids observed under low-salt conditions and often had angular features that are not generally observed in toroidal DNA structures; some even exhibit five distinct edges and a pentagonal shape (Figure 1C). TEM images also revealed variations in the intensity of the super toroids, suggesting that DNA packing was not uniform throughout these particles. To the best of our knowledge, such structures have not been previously reported.

To determine which differences between the low-salt condensates (Figure 1A) and the condensates prepared in the presence of $MgCl_2$ (Figure 1B,C) are due to equilibrium versus nonequilibrium effects of $MgCl_2$ on DNA condensation, the three condensation reactions described above were

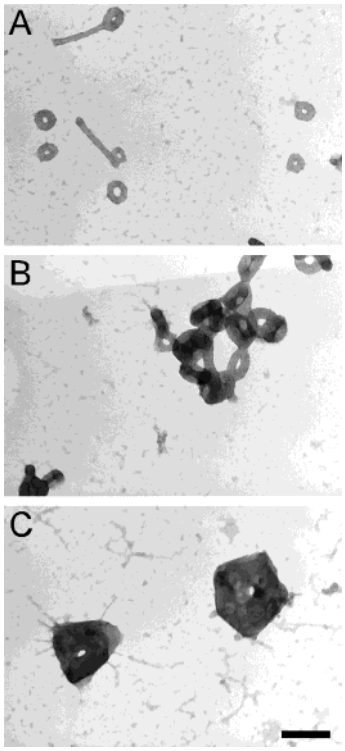

FIGURE 1: Transmission electron microscopy (TEM) images of DNA condensates formed at 22 °C by the addition of hexammine cobalt chloride. Panel A shows DNA condensed from a low-salt solution (1× TE; 10 mM Tris, 1.0 mM EDTA) by mixing with an equal volume solution of 200 μM hexammine cobalt chloride. Panel B shows DNA condensed from a solution of 3.5 mM $MgCl_2$, 1× TE by mixing with an equal volume solution of 200 μM hexammine cobalt chloride. Panel C shows DNA condensed from a low-salt solution by mixing with an equal volume solution of 200 μM hexammine cobalt chloride, 3.5 mM $MgCl_2$. DNA was a linearized form of the bacterial plasmid Bluescript II SK− (Experimental Procedures). DNA concentration in all samples was 10 μg/mL following mixing with the hexammine cobalt chloride solutions. All images are shown at the same magnification. Scale bar is 200 nm.

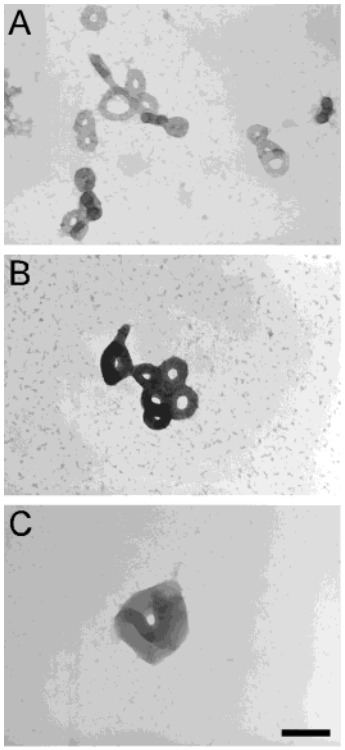

FIGURE 2: TEM images of DNA condensed at 22 °C by the addition of hexammine cobalt chloride, followed by dilution with either dH_2O or a $MgCl_2$ solution. Panel A shows DNA condensates produced under low-salt conditions (1× TE) followed by dilution with an equal volume of 1.75 mM $MgCl_2$. The condensates of this sample prior to dilution are shown in Figure 1A. Panel B shows DNA condensed from a solution of 3.5 mM $MgCl_2$ and 1× TE by mixing with an equal volume solution of 200 μM hexammine cobalt chloride, followed by dilution with an equal volume of dH_2O. The condensates of this sample prior to dilution are shown in Figure 1B. Panel C shows DNA condensed from a low-salt solution by mixing with an equal volume solution of 200 μM hexammine cobalt chloride and 3.5 mM $MgCl_2$, followed by dilution with an equal volume of dH_2O. The condensates of this sample prior to dilution are shown in Figure 1C. All condensate solutions contained a final concentration of 5 μg/mL DNA, 50 μM hexammine cobalt chloride, and 0.87 mM $MgCl_2$. Scale bar is 200 nm.

diluted with either an equal volume of 1.75 mM $MgCl_2$ (for the low-salt sample) or dH_2O (for the samples containing $MgCl_2$) so that the final composition of all three samples were identical (Experimental Procedures). The thickness and outside diameter of the toroids prepared in the absence of $MgCl_2$ (i.e., low-salt toroidal condensates) increased slightly upon the addition of $MgCl_2$ (mean thickness of 28 nm and mean diameter of 78 nm increased to 32 and 90 nm, respectively; Figure 2A). An increase in toroid aggregation was also observed (Figure 2A). Although many of the toroids within these small aggregates remained as distinct toroids, it was evident that there were some regions where the DNA strands of the toroids were intertwined with each other (Figure 2A), similar to those produced when $MgCl_2$ was preassociated with DNA (Figure 1B).

The samples containing $MgCl_2$ at the time of DNA condensation, either preassociated with DNA (Figure 1B) or added concurrently with hexammine cobalt chloride (Figure 1C), were diluted with dH_2O to produce solutions identical in chemical composition to the low-salt condensates after dilution with a $MgCl_2$ solution. A comparison between the condensates of Figure 1B and those of Figure 2B, as well as those of Figure 1C and those of Figure 2C, illustrates the effect of diluting hexammine cobalt(III) and Mg(II) by a factor of 2 after DNA has been condensed. The similarities between the same samples before and after dilution indicate that condensate size and morphology were essentially unchanged by dilution.

The DNA condensates shown in Figure 2 are from three solutions of identical chemical composition. Thus, any differences observed among these DNA condensates are purely the result of the *order* in which Mg(II) was added to each sample with respect to hexammine cobalt(III). It is clear from these images that the overall morphology and particle size of DNA condensates is largely determined by a nonequilibrium process, which is substantially altered by the presence of Mg(II).

It is important to note that the DNA used in the present study was linearized by *Hin*dIII, an endonuclease that produces a staggered cut with a four base overhang (i.e., sticky ends). Previous studies have shown that divalent cations increase the association of sticky ends in solution and thereby enhance the formation of DNA concatamers (*34*, *35*). To investigate the possibility that concatenation by end association causes toroid aggregation in samples preassociated with Mg(II), the same DNA used in this study was

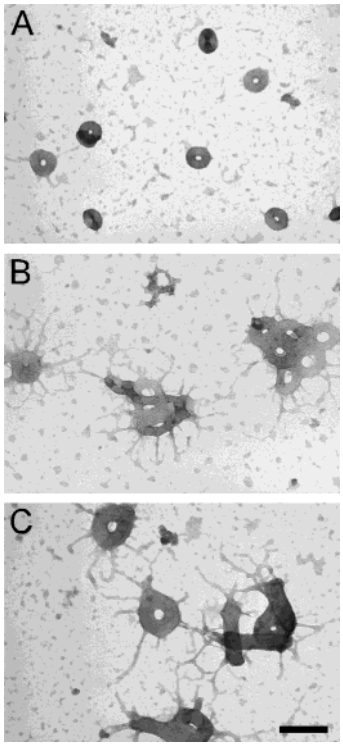

FIGURE 3: TEM images of DNA condensates formed at 37 °C by the addition of hexammine cobalt chloride. Panel A shows DNA condensed from a low-salt solution (1× TE; 10 mM Tris, 1.0 mM EDTA) by mixing with an equal volume solution of 200 μM hexammine cobalt chloride. Panel B shows DNA condensed from a solution of 3.5 mM $MgCl_2$ and 1× TE by mixing with an equal volume solution of 200 μM hexammine cobalt chloride. Panel C shows DNA condensed from a low-salt solution by mixing with an equal volume solution of 200 μM hexammine cobalt chloride and 3.5 mM $MgCl_2$. DNA was from the same stock solutions as that of Figure 1. Scale bar is 200 nm.

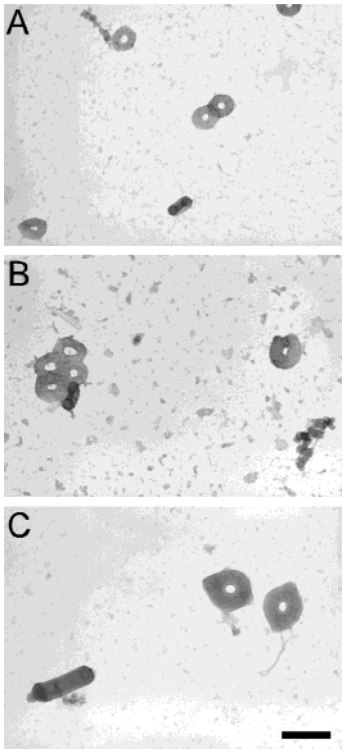

FIGURE 4: TEM images of DNA condensates produced at 37 °C by the addition of hexammine cobalt chloride to DNA, followed by dilution with either $MgCl_2$ or dH_2O. Panel A shows toroids observed from the low-salt condensate mixture when diluted with an equal volume of 1.75 mM $MgCl_2$. The condensates of this sample prior to dilution are shown in Figure 3A. Panel B shows toroids from condensation of the DNA−3.5 mM $MgCl_2$ mix diluted with an equal volume of dH_2O. The condensates of this sample prior to dilution are shown in Figure 3B. Panel C shows toroids condensed from the low-salt DNA and the hexammine cobalt chloride−3.5 mM $MgCl_2$ mixture. The condensates formed prior to dilution of these samples are shown in Figure 3C. All solutions contained a final concentration of 5 μg/mL DNA, 50 μM hexammine cobalt chloride, and 0.87 mM $MgCl_2$. Scale bar is 200 nm.

linearized with the blunt-end cutting endonuclease *Sca*I (New England Biolabs) and then condensed using protocols identical to the preassociated Mg(II) sample. The toroids produced by these experiments closely resembled those produced by DNA cut with *Hin*dIII (data not shown). Thus, the aggregation of toroids produced by the condensation of *Hin*dIII-digested DNA cannot be attributed to the presence of sticky ends.

A Small Temperature Increase Can Alter Condensate Size and Morphology. To gain additional insight into the origin of Mg(II) effects on DNA condensation, the condensation reactions described above were also performed at 37 °C. Toroids formed under low-salt conditions at 37 °C are similar to the low-salt toroids formed at 22 °C in that the vast majority of toroids observed were single toroids (Figure 3A). However, toroids formed under low-salt conditions at 37 °C are thicker than those formed at 22 °C (mean thickness of 35 vs 28 nm) and have a larger outside diameter (mean diameter of 87 vs 77 nm) (Figure 3A).

An equal volume of 1.75 mM $MgCl_2$ was added to the low-salt condensates formed at 37 °C, with all solutions being constantly maintained at 37 °C, to bring the reaction mixture to the same chemical composition as the diluted DNA condensate solutions prepared at 22 °C. This addition of divalent cations, along with sample dilution, did not alter the size of the condensates significantly, and no additional aggregation was observed (Figure 4A). These results differ from those at 22 °C, where variations in particle size and degree of aggregation were observed upon the addition of $MgCl_2$ (Figure 2A).

Small aggregates of toroids were almost exclusively observed when DNA preassociated with Mg(II) was condensed at 37 °C (Figure 3B), as was the case for DNA condensation by the same protocol at 22 °C (Figure 1B). However, the DNA of toroids produced at 37 °C were not as well condensed as the DNA of toroids produced at 22 °C. All toroids formed at 37 °C from DNA preassociated with Mg(II) have DNA fibrils extending in a radial fashion (Figure 3B). This less-condensed state of DNA is a combined result of an increase in temperature and the presence of Mg(II) during condensation, because toroids formed at 37 °C in the absence of Mg(II) (Figure 3A) or toroids formed at 22 °C in the presence of Mg(II) (Figure 1B) did not exhibit appreciable DNA fibrils.

A 2-fold dilution with dH_2O produced a dramatic change in the DNA condensates formed at 37 °C from DNA preassociated with Mg(II) (Figure 4B). The DNA fibrils protruding from toroids in these samples completely disappear upon dilution (Figure 4B). However, toroids remain locked in small aggregates. These observations suggest that the DNA fibrils extending from toroids prior to dilution condense onto toroids upon sample dilution.

The effects of increased temperature were most obvious for condensates produced when DNA in the low-salt buffer was condensed by the concurrent addition of hexammine cobalt chloride and $MgCl_2$ at 37 °C (Figure 3C). The condensates produced by this protocol at 37 °C were more typical than the super toroids produced by the same protocol at 22 °C (Figure 1C). The TEM images also revealed a marked increase in the quantity of DNA fibrils protruding from these toroids (Figure 3C), which were essentially absent from the super toroids produced at 22 °C (Figure 1C). The appearance of fibrils when DNA was condensed at 37 °C by the concurrent addition of hexammine cobalt chloride and $MgCl_2$ again indicates that both Mg(II) and increased temperature contribute to the appearance of DNA fibrils.

The DNA of condensates formed at 37 °C by the concurrent addition of hexammine cobalt chloride and $MgCl_2$ followed by dilution with an equal volume of dH_2O were more completely condensed as indicated by the disappearance of fibrils that extended from toroids prior to dilution (Figures 3C and 4C). This observation also suggests that dilution facilitates the incorporation of fibrils onto toroids. Condensates produced by the concurrent addition of hexammine cobalt chloride and $MgCl_2$ remained as individual toroids upon dilution with dH_2O and were appreciably larger in outer diameter and thickness (Figure 4C) than the aggregated toroids produced by the condensation of DNA preassociated with Mg(II) (Figure 4B). Additionally, toroids produced by the concurrent addition of hexammine cobalt chloride and $MgCl_2$ are less circular than those produced by preassociation with Mg(II) and appear to be pinched at two points approximately 180° from each other (Figure 4C). Toroids with these features occurred frequently in our preparations when hexammine cobalt chloride and $MgCl_2$ were added simultaneously to the low-salt DNA at 37 °C.

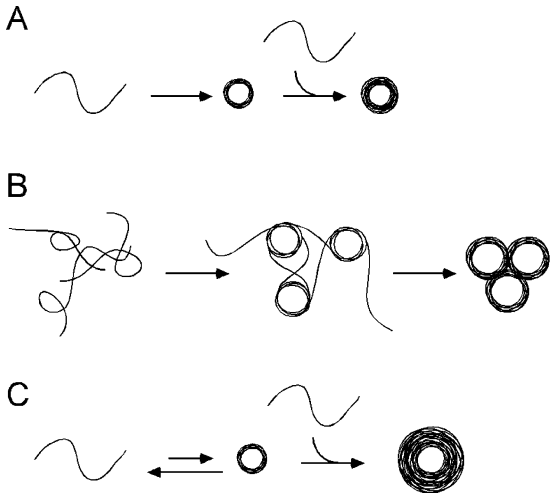

FIGURE 5: Models for the condensation of DNA by hexammine cobalt(III) under various conditions. Panel A depicts DNA condensation by a nucleation−growth pathway. DNA is well dispersed in solution and spontaneously forms nucleation loops that are stabilized by the addition of hexammine cobalt(III). The addition of DNA strands to the growning toroid continues until free DNA is depleted from solution. DNA condensation under low-salt conditions is expected to follow this pathway. Panel B depicts DNA condensation with preassociated Mg(II). Intra- and intermolecular helix−helix contacts are stabilized by the presence of Mg(II). Upon addition of hexammine cobalt chloride, both forms of helix−helix contacts nucleate DNA condensation. The resulting condensates are primarily intertwined aggregates of toroids. Panel C depicts DNA condensation from a low-salt solution by the concurrent addition of hexammine cobalt chloride and $MgCl_2$. Without Mg(II) preassociation, DNA is well dispersed in the low-salt buffer. The addition of hexammine cobalt chloride promotes DNA condensation. However, competition between Mg(II) and hexammine cobalt(III) for association with DNA reduces the stability of nucleated toroids. The fewer successfully nucleated toroids grow larger in comparison to condensation in the absence of Mg(II).

DISCUSSION

DNA toroid formation is known to be a nucleation−growth phenomenon (*19*, *36*, *37*). This implies that toroid size can be governed by both kinetic and thermodynamic factors. If toroid nucleation is rapid (i.e., occurs simultaneously throughout the solution) and association of DNA strands onto a growing toroid is always favorable (e.g., regardless of toroid size), then toroid size will be initially determined by the kinetics of condensation (Figure 5A) (*38*). That is, nucleated toroids will only stop growing when all DNA in the solution is condensed. The more frequently toroid nucleation occurs within a solution, the smaller the resulting toroids will be. If DNA strands do not exchange with solution once they have been condensed into toroids, then toroid size will be solely determined by the kinetics of nucleation and growth and the condensed DNA may not represent a minimum energy state.

Under most solution conditions, a net electrostatic charge is expected to accumulate on a DNA toroid as it increases in size because the negative charges of DNA within the toroid will not be perfectly compensated by associated cations (i.e., undercharging) (*21*−*24*, *29*, *30*, *39*, *40*). If toroid nucleation is slow compared to toroid growth, then the net negative charge of an individual toroid could eventually reach a point at which it is energetically unfavorable for additional DNA to add to the toroid, even though uncondensed DNA remains in solution. In this case, undercharging would be the primary physical parameter governing toroid size (*41*). Even under conditions where the condensation of DNA onto a growing toroid is energetically favorable, undercharging could significantly slow the kinetics of DNA deposition onto the growing toroids and thereby regulate toroid size (*29*). Under such conditions, toroid size would be governed by both thermodynamic factors and the kinetics of toroid nucleation and growth. If DNA strands remain in equilibrium exchange with solution after their initial condensation into toroids, then the repartitioning of DNA between individual toroids would eventually result in the existence of toroids with dimensions that are under thermodynamic control (*29*). At very high multivalent cation concentrations, it is also theoretically possible that the charges of DNA can be over compensated by multivalent cations such that a net positive charge accumulates on DNA condensate particles (i.e., overcharging), which should likewise lead to a limit on condensate dimensions (*21*−*24*, *29*, *30*, *39*, *40*). However, overcharging has only been observed experimentally for double-stranded DNA while associated within nucleosome core particles (*26*, *28*).

Low-Salt Toroid Size Is Kinetically Determined. If toroid size in our low-salt DNA solution was limited by undercharging, then undercharging would limit growth at an even earlier stage of toroid formation in the condensation reactions that contain $MgCl_2$ due to competition between Mg(II) and hexammine cobalt(III) for association with DNA (*42*, *43*). However, it was observed that the toroids of preparations

containing $MgCl_2$ are significantly larger than those of the low-salt preparations (Figure 1). Thus, DNA undercharging *cannot* be the size-determining factor for the low-salt toroids. DNA overcharging can also be ruled out as a limit to toroid growth because the conditions of all condensation reactions of the present study are far from the realm of conditions necessary for overcharging to occur (*26*, *28*). Thus, the size of low-salt toroids must be kinetically determined; otherwise, the low-salt toroids would grow to be at least as large as toroids in the condensation reactions that contained $MgCl_2$.

The formation of super toroids by the concurrent addition of $MgCl_2$ and hexammine cobalt chloride to low-salt DNA can be attributed to an alteration in the kinetics of toroid growth by Mg(II) (*38*). The presence of Mg(II) during the initiation of DNA condensation will reduce the frequency of toroid nucleation because the competition between Mg(II) and hexammine cobalt(III) for DNA will weaken the helix−helix associations that are promoted by hexammine cobalt(III) (*42*, *43*). For certain concentrations of $MgCl_2$ and hexammine cobalt chloride (e.g., those selected for this study), successful toroid nucleation may only occur when several DNA molecules simultaneously condense to form a prototoroid with the minimum number of helix−helix contacts necessary for stability in the presence of Mg(II) (*41*). With less frequent nucleation, free DNA would be available in solution for a longer time after the initiation of condensation, which would allow the fewer toroids formed to grow to the size of super toroids (Figure 5C). This same explanation applies to the positive correlation that we have reported between toroid size and NaCl concentration (*19*), although the effect is not as dramatic in the case of monovalent cations. It is possible that super toroid size is ultimately limited by undercharging. This possibility is discussed further below in regards to the 37 °C data.

The fact that super toroids have holes of similar size to the low-salt toroids suggests that super toroids may be nucleated by prototoroids similar in size to the low-salt toroids (Figure 1A,C). Unfortunately, it is currently not possible to measure the size of DNA toroids as a function of time during the onset of condensation because the initial stages of condensation are too rapid to obtain toroid size information at nanometer resolution by solution-based techniques, such as light scattering (*44*, *45*).

DNA Preorganization by Mg(II) Causes Toroid Aggregation by Altering Nucleation Structures. The addition of $MgCl_2$ to DNA prior to condensation resulted in the production of toroid aggregates (Figure 1B), in contrast to the predominance of single toroids observed when $MgCl_2$ was not present or was added concurrently with hexammine cobalt chloride (Figure 1A,C). The presence of an alternative nucleation structure for DNA samples with preassociated Mg(II) explains this observation. It has been previously demonstrated that divalent cations promote DNA helix−helix contacts in solution (*46*−*50*) but not to the extent necessary for condensation. Consequently, the addition of $MgCl_2$ to DNA samples prior to condensation would be expected to promote an appreciable number of intramolecular helix−helix contacts (e.g., DNA loops) and intermolecular helix−helix contacts along 3 kb DNA (Figure 5B). Upon the addition of hexammine cobalt chloride, these preformed structures would act as nucleation sites for DNA condensation (*18*, *36*). Mg(II)-stabilized DNA loops would nucleate toroid formation, whereas Mg(II)-stabilized intermolecular helix−helix contacts could result in the cocondensation of DNA strands onto different toroids at different points along their lengths. Thus, the existence of precondensation helix−helix contacts would promote the rapid formation of intertwined toroids, ultimately producing networks of toroids that are impossible to separate without complete decondensation of the DNA (Figure 5B). We propose that this is the origin of the toroid aggregates observed upon the condensation of DNA with preassociated Mg(II).

If the concurrent addition of $MgCl_2$ with hexammine cobalt chloride can produce super toroids (Figure 5C), then we must question why DNA samples with preassociated Mg(II) produce significantly smaller toroids. This can also be explained as a result of the kinetic path taken during DNA condensation. As we mentioned above, the preassociation of Mg(II) with DNA will lead to the formation of intra- and intermolecular helix−helix contacts (Figure 5B). These contacts could cause the formation of toroidal aggregates to be rapid compared to the rate of strand rearrangement that would be necessary for the production of super toroids. In other words, the preassociation of Mg(II) leads to the formation of intertwined toroids that act as kinetic traps, which makes the formation of super toroids extremely rare. Two additional observations support this explanation. First, we have observed a single super toroid amid an EM grid of smaller aggregated toroids from a condensation reaction of DNA preassociated with Mg(II) (data not shown). This is consistent with a kinetic component contributing to the origin of aggregate formation. Second, when higher concentrations of $MgCl_2$ are preincubated with DNA, the toroids produced upon condensation are not aggregated (*19*). This observation would support an increase in competition between Mg(II) and hexamine cobalt(III) allowing DNA in the early stages of condensation to pass over the kinetic barriers presented by entangled structures and to rearrange into (presumably) more efficiently packed single toroids.

Polymer Exchange between Toroids Is Limited. Adding $MgCl_2$ to the low-salt toroid preparation increased the average outer diameter of toroids by 13 nm (i.e., from 77 to 90 nm) and caused a substantial increase in toroid aggregation (Figure 2A). Both of these changes can be explained by DNA strand exchange occurring between toroids after the addition of $MgCl_2$. The release of DNA from some toroids upon the introduction of $MgCl_2$ could lead to complete decondensation of some (particularly smaller) toroids, thereby reintroducing free DNA into solution that subsequently contributes to the growth and stabilization of other toroids. Similarly, aggregation could come about by the equilibrium exchange of DNA strands between toroids, which causes some toroids to become associated by strand sharing. In any case, the changes resulting from the addition of $MgCl_2$ to the low-salt condensates represent a shift in the size and degree of aggregation closer to that observed when Mg(II) is preassociated with DNA (Figure 2B). However, it is clear that the DNA strands of toroids are not entirely free to exchange with solution, because the addition of $MgCl_2$ to low-salt toroids (Figure 2A) does not result in toroid growth to the same size or aggregation state as those formed in the presence of $MgCl_2$ (Figure 2B,C). These combined results again illustrate that toroid size can be highly dependent on the path taken by DNA during condensation.

Comparison of DNA Condensed at Different Temperatures Illustrates Both Thermodynamic and Kinetic Limits to Toroid

Growth. DNA condensation has been shown to be a result of dynamic correlations between multivalent cations that are associated with DNA strands in close proximity (*5*, *20*, *21*). This attractive potential decreases with increasing temperature (*21*, *31*, *51*−*54*). Thus, under conditions where toroid size is primarily limited by thermodynamic factors, toroid size would be expected to decrease with increasing temperature. On the other hand, if toroid size is primarily limited by the kinetics of growth, then toroid size should initially increase with increasing temperature because toroid nucleation will be less favored at higher temperatures. We have observed that the concurrent addition of $MgCl_2$ and hexammine cobalt chloride to DNA at 37 °C produces single toroids that are considerably smaller and greater in number than the super toroids produced by the same condensation protocol at 22 °C (Figure 3C). This observation indicates that at 37 °C toroid size is limited by a thermodynamic parameter (i.e., undercharging) rather than the kinetics of nucleation and growth.

Our conclusion that the size of low-salt toroids is kinetically determined is also consistent with our observation that low-salt toroids produced at 37 °C are larger (mean diameter 87 nm, mean thickness 35 nm) than those produced under low-salt conditions at 22 °C (mean diameter 77 nm, mean thickness 28 nm) (Figures 1A and 3A). Thus, under the low-salt conditions, the reduction in DNA helix−helix attraction potential upon raising the temperature from 22 to 37 °C must reduce the probability of toroid nucleation enough to allow successfully nucleated toroids at 37 °C to grow measurably larger than those produced at 22 °C.

When the temperature of condensation was increased to 37 °C abundant DNA fibrils were observed protruding from the toroids produced by the condensation of DNA in the presence of $MgCl_2$ (Figure 3B,C). We propose that these fibrils result from uncondensed loops of DNA that protrude from the surfaces of toroids in solution and that these loops collapse into fibrils upon preparation of EM grids. This proposal is based upon two previous reports. First, atomic force microscopy (AFM) studies of DNA condensates in solution have revealed DNA loops protruding from a more condensed core particle under conditions where DNA condensation was incomplete (*55*). Second, a previous study by cryo-TEM has demonstrated that staining with uranyl acetate facilitates DNA condensation (*56*). Thus, it is reasonable that if a toroidal condensate has loops of DNA protruding from its surface when deposited on an EM grid, then the subsequent addition of uranyl acetate (and rinsing by ethanol) would cause these loops to condense into fibrils. These loops may appear because toroids prepared at 37 °C are at their maximum limit of growth due to undercharging and DNA strands added to those toroids during the final stage of growth remain only partially condensed. If this is truly the case, then the DNA condensates produced in the presence of $MgCl_2$ at 37 °C are governed by both kinetic and thermodynamic factors, because condensation under purely thermodynamic control would be expected to allow the partially condensed DNA to release into solution and form slightly smaller toroids with completely condensed DNA.

Upon dilution with water, fibrils extending from condensates prepared in the presence of $MgCl_2$ at 37 °C (Figure 3B,C) are no longer observed, as all DNA particles appear to be fully condensed with clearly defined edges (Figure 4B,C). This observation provides additional support for our hypothesis that at 37 °C the fibrils are indicative of some DNA associated with each toroid remaining partially uncondensed. Based upon the formalism derived by Rouzina and Bloomfield to calculate the surface concentration of cations around DNA as a function of cation valence and bulk concentration (*42*, *43*), dilution by a factor of 2 of the condensation reactions in this study would appreciably increase the DNA charge neutralized by trivalent hexammine cobalt(III) over divalent Mg(II), even though the relative concentration of these cations in solution remains constant. Thus, sample dilution would be expected to enhance DNA condensation, which causes the DNA loops to condense onto the toroids in an ordered fashion prior to EM grid preparation.

CONCLUSIONS

The results presented here demonstrate that the size of DNA toroids can be governed by both thermodynamic and kinetic factors. Under our low-salt conditions we have concluded that toroid size is primarily limited by the kinetics of toroid nucleation and growth. Understanding the size and morphology of DNA condensates prepared in the presence of $MgCl_2$, on the other hand, requires the consideration of both kinetic and thermodynamic factors. When $MgCl_2$ is added to DNA prior to condensation, Mg(II)-stabilized helix−helix contacts provide a means to kinetically trap DNA into aggregate structures that are unable to rearrange into what are presumably lower-energy structures. The influence of these kinetic traps in limiting toroid size is illustrated by the observation that the concurrent addition of $MgCl_2$ and hexammine cobalt chloride allows the formation of super toroids. The dominance of thermodynamic limits on toroid size when $MgCl_2$ and hexammine cobalt chloride are added concurrently to DNA is supported by the fact that toroids decrease in size if the temperature is increased at the time of condensation. We have also demonstrated that DNA strand exchange between toroids can be very limited, because three condensate samples that only differ in regards to the step at which $MgCl_2$ is added maintain very different condensate structures. All together our results clearly illustrate that DNA condensates are not likely, in many cases, to represent equilibrium structures.

ACKNOWLEDGMENT

We thank Igor D. Vilfan for helpful discussions and the reviewers of this manuscript for their helpful comments. We also thank the Georgia Institute of Technology Electron Microscopy Center for use of its JEOL-100C and Ms. Yolande Berta for technical assistance.

REFERENCES

1. Gosule, L. C., and Schellman, J. A. (1976) Compact form of DNA induced by spermidine, *Nature 259*, 333−335.
2. Gosule, L. C., and Schellman, J. A. (1978) DNA condensation with polyamines I. Spectroscopic studies, *J. Mol. Biol. 121*, 311−326.
3. Chattoraj, D. K., Gosule, L. C., and Schellman, J. A. (1978) DNA condensation with polyamines. II. Electron microscopic studies, *J. Mol. Biol. 121*, 327−337.
4. Widom, J., and Baldwin, R. L. (1980) Cation-induced toroidal condensation of DNA studies with $Co^{3+}(NH_3)_6$, *J. Mol. Biol. 144*, 431−453.
5. Bloomfield, V. (1996) DNA Condensation, *Curr. Opin. Struct. Biol. 6*, 334−341.
6. Bloomfield, V. (1997) DNA condensation by multivalent cations, *Biopolymers 44*, 269−282.

7. Hud, N. V., and Downing, K. H. (2001) Cryoelectron microscopy of lambda phage DNA condensates in vitreous ice: The fine structure of DNA toroids, *Proc. Natl. Acad. Sci. U.S.A. 98*, 14925−14930.
8. Rolland, A. (1998) From genes to gene medicines: recent advances in nonviral gene delivery, *Crit. Rev. Ther. Drug Carrier Syst. 15*, 143−198.
9. Mahato, R., Smith, L., and Rolland, A. (1999) *Advances in Genetics*, pp 95−155, Academic Press, New York.
10. Plank, C., Tang, M. X., Wolfe, A. R., and Szoka, F. C., Jr. (1999) Branched cationic peptides for gene delivery: Role of type and number of cationic residues in formation and in vitro activity of DNA polyplexes, *Hum. Gene Ther. 10*, 319−332.
11. Luo, D., and Saltzman, W. (2000) Synthetic DNA delivery systems, *Nat. Biotech. 18*, 33−37.
12. Vijayanathan, V., Thomas, T., and Thomas, T. J. (2002) DNA nanoparticles and development of DNA delivery vehicles for gene therapy, *Biochemistry 41*, 14085−14094.
13. Reich, Z., Ghirlando, R., and Minsky, A. (1992) Nucleic acids packaging process: Effects of adenine tracts and sequence-dependent curvature, *J. Biomol. Struct. Dyn. 9*, 1097−1109.
14. Reich, Z., Levin-Zaidman, S., Gutman, S. B., Arad, T., and Minsky, A. (1994) Supercoiling-regulated liquid-crystalline packaging of topologically constrained, nucleosome-free DNA molecules, *Biochemistry 33*, 14177−14184.
15. Ma, C., and Bloomfield, V. A. (1994) Condensation of supercoiled DNA induced by $MnCl_2$, *Biophys. J. 67*, 1678−1681.
16. Ma, C., Sun, L., and Bloomfield, V. A. (1995) Condensation of plasmids enhanced by Z-DNA conformation of $d(CG)_n$ inserts, *Biochemistry 34*, 3521−3528.
17. Schnell, J. R., Berman, J., and Bloomfield, V. A. (1998) Insertion of telomere repeat sequence decreases plasmid DNA condensation by cobalt (III) hexaammine, *Biophys. J. 74*, 1484−1491.
18. Shen, M., Downing, K., Balhorn, R., and Hud, N. (2000) Nucleation of DNA condensation by static loops: Formation of DNA toroids with reduced dimensions, *J. Am. Chem. Soc. 122*, 4833−4834.
19. Conwell, C. C., Vilfan, I. D., and Hud, N. V. (2003) Controlling the size of nanoscale toroidal DNA condensates with static curvature and ionic strength, *Proc. Natl. Acad. Sci. U.S.A. 100*, 9296−9301.
20. Strey, H. H., Podgornik, R., Rau, D. C., and Parsegian, V. A. (1998) DNA-DNA interactions, *Curr. Opin. Struct. Biol. 8*, 309−313.
21. Gelbart, W. M., Bruinsma, R. F., Pincus, P. A., and Parsegian, V. A. (2000) DNA-Inspired Electrostatics, *Phys. Today 53*, 38−44.
22. Park, S. Y., Bruinsma, R. F., and Gelbart, W. M. (1999) Spontaneous overcharging of macro-ion complexes, *Europhys. Lett. 46*, 454−460.
23. Shklovskii, B. I. (1999) Screening of a macroion by multivalent ions: Correlation-induced inversion of charge, *Phys. Rev. E 60*, 5802−5811.
24. Nguyen, T. T., Rouzina, I., and Shklovskii, B. I. (2000) Reentrant condensation of DNA induced by multivalent counterions, *J. Chem. Phys. 112*, 2562−2568.
25. Raspaud, E., Olvera de la Cruz, M., Sikorav, J.-L., and Livolant, F. (1998) Precipitation of DNA by polyamines: A polyelectrolyte behavior, *Biophys. J. 74*, 381−393.
26. Raspaud, E., Chaperon, I., Leforstier, A., and Livolant, F. (1999) Sperimine-induced aggregation of DNA, nucleosome, and chromatin, *Biophys. J. 77*, 1547−1555.
27. Trubetskoy, V. S., Loomis, A., Hagstrom, J. E., Budker, V. G., and Wolff, J. A. (1999) Layer-by-layer deposition of oppositely charged polyelectrolytes on the surface of condensed DNA particles, *Nucleic Acids Res. 27*, 3090−3095.
28. de Fructos, M., Raspaud, E., Leforstier, A., and Livolant, F. (2001) Aggregation of nucleosomes by divalent cations, *Biophys. J. 81*, 1127−1132.
29. Nguyen, T. T., and Shklovskii, B. I. (2002) Kinetics of macroion coagulation induced by multivalent counterions, *Phys. Rev. E 65*, 031409-1−031409-7.
30. Levin, Y., and Arenzon, J. J. (2003) Kinetics of charge inversion, *J. Phys. A: Math. Gen. 36*, 5857−5863.
31. Ha, B.-Y., and Liu, A. J. (1998) Effect of non-pairwise-additive interactions on bundles of rodlike polyelectrolytes, *Phys. Rev. Lett. 81*, 1011−1014.
32. Stevens, M. J. (1999) Bundle binding in polyelectrolyte solutions, *Phys. Rev. Lett. 82*, 101−104.
33. Arscott, P. G., Li, A.-Z., and Bloomfield, V. A. (1990) Condensation of DNA by trivalent cations. 1. Effects of DNA length and topology on the size and shape of condensed particles, *Biopolymers 30*, 619−630.
34. Dahlgren, P. R., and Lyubchenko, Y. L. (2002) Atomic force microscopy study of the effects of Mg^{2+} and other divalent cations on the end-to-end DNA interactions, *Biochemistry 41*, 11372−11378.
35. Revet, B., and Fourcade, A. (1998) Short unligated sticky ends enable the observation of circularised DNA by atomic force and electron microscopies, *Nucleic Acids Res. 26*, 2092−2097.
36. Hud, N. V., Downing, K. H., and Balhorn, R. (1995) A constant radius of curvature model for the organization of DNA in toroidal condensates, *Proc. Natl. Acad. Sci. U.S.A. 92*, 3581−3585.
37. Yoshikawa, K., and Matsuzawa, Y. (1996) Nucleation and Growth in Single DNA Molecules, *J. Am. Chem. Soc. 118*, 929−930.
38. LaMer, V. K., and Dinegar, R. H. (1950) Theory, production and mechanism for formation of monodispersed hydrosols, *J. Am. Chem. Soc. 72*, 4847−4854.
39. Mateescu, E. M., Jeppensen, C., and Pincus, P. (1999) Overcharging of a spherical macroion by an oppositely charged polyelectrolyte, *Europhys. Lett. 46*, 493−498.
40. Grosberg, A. Y., Nguyen, T. T., and Shklovskii, B. I. (2002) Colloquium: The physics of charge inversion in chemical and biological systems, *Rev. Mod. Phys. 74*, 329−345.
41. Bloomfield, V. A. (1991) Condensation of DNA by multivalent cations: considerations on mechanism, *Biopolymers 31*, 1471−1481.
42. Rouzina, I., and Bloomfield, V. A. (1996) Competitive electrostatic binding of charged ligands to polyelectrolyes: Planar and cylindrical geometries, *J. Phys. Chem. 100*, 4292−4304.
43. Rouzina, I., and Bloomfield, V. A. (1997) Competitive electrostatic binding of charged ligands to polyelectrolytes: Practical approach using the nonlinear Poisson−Boltzmann equation, *Biophys. Chem. 64*, 139−155.
44. Porschke, D. (1984) Dynamics of DNA condensation, *Biochemistry 23*, 4821−4828.
45. He, S., Arscott, P. G., and Bloomfield, V. A. (2000) Condensation of DNA by multivalent cations: Experimental studies of condensation kinetics, *Biopolymers 53*, 329−341.
46. Adrian, M., Heggeler-Bordier, B., Wahli, W., Stasiak, A. Z., Stasiak, A., and Dubochet, J. (1990) Direct visualization of supercoiled DNA molecules in solution, *EMBO J. 9*, 4551−4554.
47. Bednar, J., Furrer, P., Stasiak, A., Dubochet, J., Egelman, E. H., and Bates, A. D. (1994) The twist, writhe, and overall shape of supercoiled DNA change during counterion-induced transition from a loosely to a tightly interwound superhelix, *J. Mol. Biol. 235*, 825−847.
48. Kornyshev, A. A. (1999) Electrostatic zipper motif for DNA aggregation, *Phys. Rev. Lett. 82*, 4138−4141.
49. Safinya, C. R. (2001) Structures of lipid-DNA complexes: supramolecular assembly and gene delivery, *Curr. Opin. Struct. Biol. 11*, 440−448.
50. Cherny, D. I., and Jovin, T. M. (2001) Electron and scanning force microscopy studies of alterations in supercoiled DNA tertiary structure, *J. Mol. Biol. 313*, 295−307.
51. Rouzina, I., and Bloomfield, V. (1996) Macroion attraction due to electrostatic correlation between screening counterions 1. Mobile surface-adsorbed ions and diffuse ion cloud, *J. Phys. Chem. 100*, 9977−9989.
52. Gronbech-Jensen, N., Mashl, R. J., Bruinsma, R. F., and Gelbart, W. M. (1997) Counterion-induced attraction between rigid polyelectrolytes, *Phys. Rev. Lett. 78*, 2477−2480.
53. Ha, B.-Y., and Liu, A. J. (1997) Counterion-mediated attraction between two like-charged rods, *Phys. Rev. Lett. 79*, 1289−1292.
54. Ha, B.-Y., and Liu, A. J. (1999) Counterion-mediated, non-pairwise-additive attractions in bundles of like-charged rods, *Phys. Rev. E 60*, 803−813.
55. Hansma, H. G., Golan, R., Hsieh, W., Lollo, C. P., Mullen-Ley, P., and Kwoh, D. (1998) DNA condensation for gene therapy as monitored by atomic force microscopy, *Nucleic Acids Res. 26*, 2481−2487.
56. Böttcher, C., Endisch, C., Fuhrhop, J. H., Catterall, C., and Eaton, M. (1998) High-yield preparation of oligomeric C-type DNA toroids and their characterization by cryoelectron microscopy, *J. Am. Chem. Soc. 120*, 12−17.

BI049872U